

Disorder-to-Order Phase Transition and Multiple Melting Behavior of Poly(L-lactide) Investigated by Simultaneous Measurements of WAXD and DSC

Jianming Zhang,[†] Kohji Tashiro,^{*,†} Hideto Tsuji,[‡] and Abraham J. Domb[§]

Department of Future Industry-oriented Basic Science and Materials, Graduate School of Engineering, Toyota Technological Institute, Tempaku, Nagoya 468-8511, Japan; Department of Ecological Engineering, Faculty of Engineering, Toyohashi University of Technology, Toyohashi, Aichi 441-8580, Japan; and Department of Medicinal Chemistry, School of Pharmacy-Faculty of Medicine, The Hebrew University of Jerusalem, Jerusalem 91120, Israel

Received March 12, 2007; Revised Manuscript Received May 31, 2007

ABSTRACT: It has been found that, dependent on the crystallization temperature (T_c), the disorder (α') and order (α) phases of poly(L-lactide) (PLLA) are formed at low ($T_c < 100$ °C) and high ($T_c \geq 120$ °C) temperatures, respectively. In the DSC curves, the sample with α' phase demonstrates a peculiar small exothermal peak around 160 °C just prior to the melting point, while the sample crystallized at temperatures around 120 °C (between 110 and 130 °C) shows a double melting behavior. These distinct thermal behaviors of various PLLA samples were investigated in detail by simultaneous measurements of WAXD and DSC. It is confirmed that the small exothermal peak corresponds to the disorder-to-order (α' -to- α) phase transition, in which the chain packing of the crystal lattice becomes more compacted. In the process of the α' -to- α phase transition, the isosbestic points were found in the temperature-dependent WAXD profiles. So far, the α' -to- α transition was considered to occur apparently continuously as long as the main 200/110 peak was measured, but detailed investigation of higher 2θ peaks has revealed for the first time that the α' phase transforms discretely to the α phase in the first-order transition mode. On the basis of the X-ray diffraction and DSC data, a kind of phase diagram concerning the α' and α forms has been constructed reasonably.

Introduction

Poly(L-lactide) (PLLA) ($-\text{[CH(CH}_3\text{)COO]}_n-$) is a biodegradable crystalline polymer produced from renewable biomass such as corn, and it exhibits the biocompatibility and high mechanical performances comparable to those of petroleum-based traditional polymers.^{1,2} In the past decades, PLA has been applied to products such as clothes, cups, packaging, and many other everyday products. Nowadays, more advantageous applications of this environmentally friendly polymer are under development for car and computer parts, which bring forward the demand on improving the thermal and mechanical properties of the PLA-based product.

PLA homopolymer (PLLA or PDLA) is known to form three kinds of crystal modifications (α , β , and γ forms).^{3–7} Very recently, a new crystal modification named α' form (disorder α) was proposed for the PLLA sample crystallized below 120 °C, different from the order α form crystallized at higher temperature (> 120 °C).^{8,9} Existence of these two crystal forms can explain the peculiar crystallization behavior of the conventional α form:^{9–17} (1) The curve of spherulite growth rate (G) vs crystallization temperature (T_c) shows a clear deviation from the usual bell-shaped curve of polymer crystal growth, and a discontinuity is observed around 100–120 °C.^{10,11} (2) The size of spherulites crystallized above 120 °C is on the order of several hundred micrometers, while only tiny spherulites are obtained below 120 °C.^{9,11,12,16} (3) Crystal thickness and long period have minimum at around $T_c = 120$ °C and increase at both higher

and lower T_c .⁹ In this way, the recognition of the two different crystal forms α' and α can explain many kinds of observations made for the conventionally assigned α form. However, because of the high similarity in the X-ray powder diffraction pattern and IR spectra among the various PLLA samples crystallized at low and high T_c , there are still many ambiguities for the existence of the α' form of PLLA.^{10,18} In our previous paper,¹⁹ we reported for the first time the X-ray fiber patterns and polarized IR/Raman spectra which were taken successfully for the uniaxially oriented α' form of PLLA. These data gave direct evidence for the existence of the disorder α form (α'), which should be distinguished from the order α form formed at higher temperature. The preliminary analysis of these data suggests that the chain conformation and chain-packing mode of the disorder α form are different from those of order α form. The details of the structural analysis will be reported elsewhere.

Another important aspect of the α' form is about the phase transition behavior in the heating process. On the basis of temperature-dependent measurements of FTIR spectra of the unoriented α' form,⁸ a phase transition was detected around 160 °C prior to the melting, which corresponds to a small exothermic peak in DSC thermogram. However, lacking rigorous assignment of the IR bands of PLLA, it was hard to conclude that this is a “phase transition”. More clear evidence is needed to show the structural change occurring in the crystal lattice by the X-ray diffraction method. Cho et al.⁹ assigned a small peak of the DSC thermogram to the formation of regular crystals on the basis of the temperature-dependent SAXS measurement. Recently, Di Lorenzo²⁰ proposed a partial melt/recrystallization/crystal perfection mechanism for the structural reorganization of the α phase at high temperature before melting. But these interpretations have not yet been confirmed with well-established experimental evidence. Once we confirm the exist-

* To whom all correspondence should be addressed: Fax (+81) 52 809 1793; e-mail ktashiro@toyota-ti.ac.jp.

[†] Toyota Technological Institute.

[‡] Toyohashi University of Technology.

[§] The Hebrew University of Jerusalem.

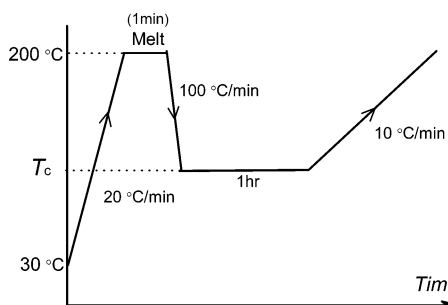


Figure 1. Thermal program employed for the DSC measurement of PLLA samples isothermally crystallized at different temperatures.

ence of the α' form, the detailed investigation of the DSC thermograms can be made on the basis of the thermal behavior of the α' form.

In the present study, a kind of phase diagram concerning the α' and α forms has been constructed reasonably on the basis of detailed wide-angle X-ray diffraction (WAXD) and DSC studies. That is, the structural changes during the heating of the various crystal modifications (α' , α , and their mixture phase) of PLLA were investigated by the simultaneous measurements of WAXD and DSC. The disorder-to-order (α' -to- α) phase transition is confirmed, and its phase transition mechanism is discussed according to the detailed investigation of higher 2θ diffraction peaks of WAXD data. The multiple melting behavior of PLLA sample has also been discussed.

Experimental Section

Samples. Synthesis and purification of the PLLA samples with various molecular weights ($M_w = 9.8 \times 10^5$, 1.5×10^5 , and 5.0×10^4 g mol $^{-1}$ and $M_w/M_n = 2.0$, 1.8, and 1.8, respectively) used in this work were performed according to the procedures reported previously.²¹

Measurements. **DSC.** The thermal behaviors of PLLA sample crystallized isothermally at various constant temperatures from the melt were investigated using a TA Instruments DSC Q1000. The thermal program employed is depicted in Figure 1. A sample was heated from 30 °C to melting temperature at a rate 20 °C/min, where it was held for 1 min, then cooled at a rate 100 °C/min to a desired crystallization temperature (T_c), and kept for 1 h for the isothermal crystallization (holding time 1 h was found to be enough to finish the crystallization in the temperature range from 85 to 150 °C). Subsequently, the crystallized sample was heated immediately to 200 °C at a rate of 10 °C/min, during which the DSC thermogram was measured. The similar procedure was made for the samples crystallized at the various constant temperatures from 85 to 150 °C.

WAXD–DSC Simultaneous Measurements. A Rigaku X-ray diffraction RINT-TTR III was used for the simultaneous measurement of WAXD and DSC in the heating process from the ambient temperature. The X-ray beam used was Cu K α radiation. The X-ray powder patterns were measured in the 2θ ranges of 5°–30°, and the heating rate was 2 °C/min.

Results and Discussion

Effect of T_c on the Thermal Behavior of PLLA. As mentioned in the Introduction, it has been found that the crystal modifications of PLLA are related to the crystallization temperature (T_c). For establishing the relationship between T_c and thermal behavior of the crystal modification in detail, the DSC thermograms of PLLA are analyzed as a function of T_c in a wide temperature region from 85 to 150 °C, which is above the T_g (≈ 58 °C) and below the melting point of PLLA (≈ 170 °C). Figure 2 shows the effect of crystallization temperature on the thermal behavior of PLLA, where three kinds

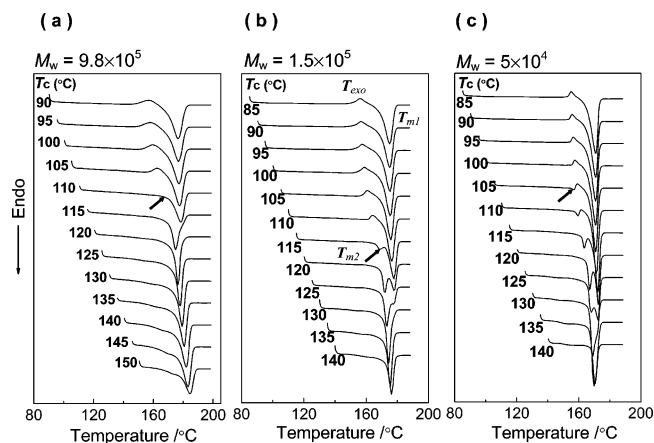


Figure 2. Effect of crystallization temperature on melting behavior of PLLA samples with different molecular weights: (a) 9.8×10^5 , (b) 1.5×10^5 , and (c) 5×10^4 g/mol.

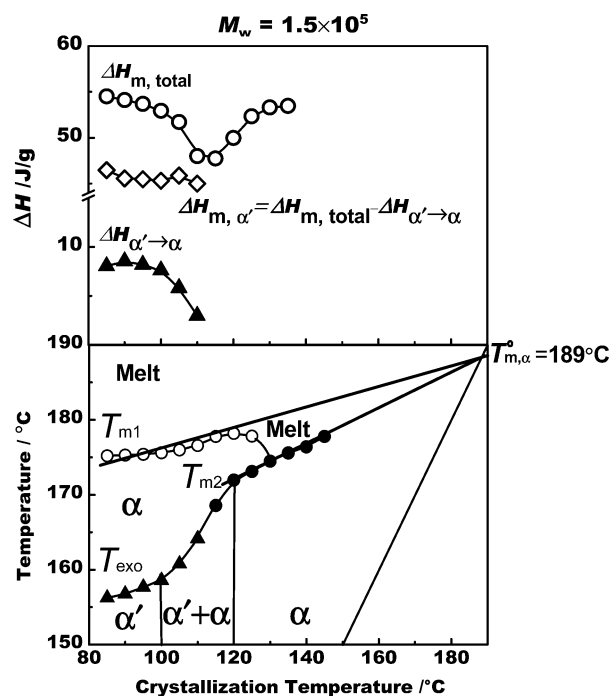


Figure 3. Enthalpy changes ΔH and the melting and transition temperatures plotted as a function of crystallization temperature.

of samples with different molecular weights were examined. The thermal behaviors of all these samples show essentially the same T_c dependence. Three kinds of distinct melting behaviors could be identified with increasing T_c from 85 to 150 °C. As an example, the typical thermal behavior investigated for the sample with middle molecular weight (1.5×10^5 g mol $^{-1}$) is described here. When $T_c < 110$ °C, the DSC curve is characterized by a small exothermic peak (denoted as T_{exo}) prior to the melting peak (T_{m1}). When 110 °C $< T_c < 130$ °C, the small exothermal peak disappears, and an additional melting peak (T_{m2}) is observed. The peak height of T_{m2} relative to T_{m1} increases with increasing T_c . At $T_c > 130$ °C, only a single melting peak (T_{m2}) appears. The enthalpy change in the melting (ΔH_m), the small exothermic enthalpy ($\Delta H_{\alpha' \rightarrow \alpha}$), and the peak positions of T_{m1} , T_{m2} , and T_{exo} are plotted against the crystallization temperature, as shown in Figure 3.

T_{exo} behaves in a different manner from T_{m1} and T_{m2} . As will be clarified later by the X-ray diffraction measurement, the α' form transfers to the α form at T_{exo} . Both the T_{m1} and T_{m2} are considered to relate with the melting phenomenon of the α form.

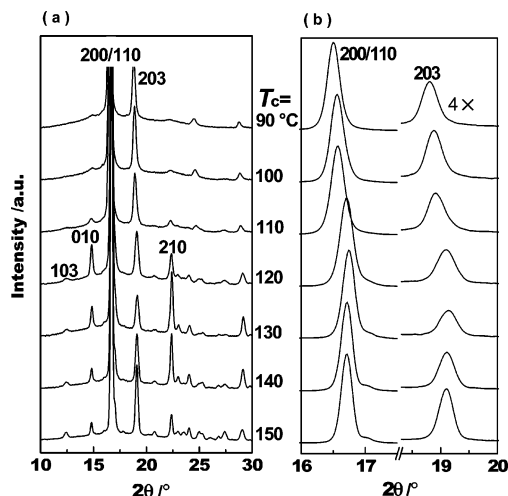


Figure 4. Powder diffraction patterns measured at room temperature for PLLA samples melt-crystallized at different temperatures.

They merge into one point by extrapolating into a straight line $T_m = T_c$, giving an equilibrium melting point of ca. 189 °C according to the Hoffman–Weeks equation.²² The linear relation shows that α phase is formed at $T_c \geq 120$ °C. A similar relation is obtained also for the samples given in Figure 2a,c: the equilibrium temperature is 198 °C for the sample with $M_w = 9.8 \times 10^5$ g mol⁻¹ and 178 °C for the sample with $M_w = 5.0 \times 10^4$ g mol⁻¹.

It should be noticed here that the ΔH_m shows a minimum around 110 °C and increases for both higher and lower T_c . It is easy to understand that the ΔH_m increases with increasing T_c because the crystallinity is usually improved by annealing at higher temperature. However, at $T_c < 110$ °C, a peculiar decrease of ΔH_m is observed with increasing T_c . This is similar to the T_c dependence of $\Delta H_{\alpha' \rightarrow \alpha}$. Because the disorder α phase obtained at low T_c (<110 °C) reorganizes into the order α phase in the heating process, the final melting enthalpy does not represent the initial crystallinity of the starting material (α'). The melting enthalpy of α' form in the starting sample crystallized below 110 °C may be evaluated by the following equation:

$$\Delta H_{m,\alpha'} = \Delta H_m - \Delta H_{\alpha' \rightarrow \alpha}$$

The result depicted in Figure 3 shows that $\Delta H_{m,\alpha'}$ remains almost unchanged with increasing T_c below 110 °C and is lower than the ΔH_m obtained above 110 °C. That is to say, the crystallinity of PLLA sample crystallized at T_c below 110 °C is kept constant and smaller than those crystallized at higher temperature (>110 °C). The decrease in $\Delta H_{\alpha' \rightarrow \alpha}$ with increasing T_c may be ascribed to at least two reasons: (i) the decreases in α' content included in the sample crystallized at relatively high temperature and (ii) the gradual improvement of crystal regularity during annealing at higher T_c . The X-ray diffraction data support these factors explicitly, as discussed in the next section.

X-ray Diffraction Patterns of PLLA Crystallized at Different T_c . The WAXD patterns of unoriented PLLA samples crystallized at various T_c s are shown in Figure 4a. For comparison, all the diffraction patterns given there are normalized using the strongest 200/110 reflection intensity. Indexing of the observed reflections is based on the crystal structure reported for the order α .^{23–25} As seen in these profiles, the relative intensities of the X-ray reflection peaks are not necessarily the same among the samples crystallized at the various T_c , probably due to the preferential orientation of the

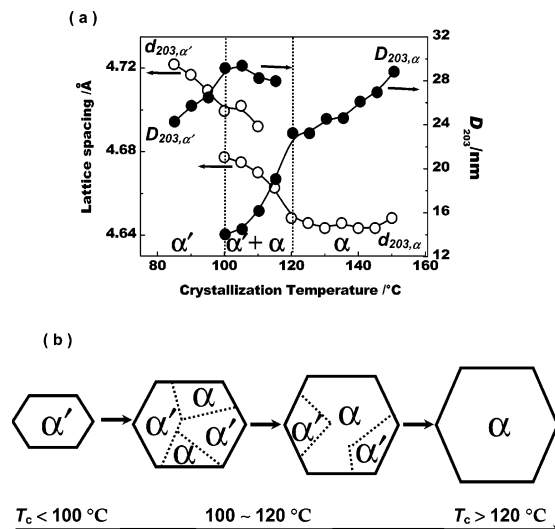


Figure 5. (a) Lattice spacing (open circle) and crystal size (solid circle) as a function of crystallization temperature derived from 203 reflection in Figure 4. (b) Proposed model for the crystal modifications acquired under various crystallization temperatures.

crystallites which depends more or less on the sample history. The two strong reflections of 200/110 and 203 are observed for all the samples. Several reflections such as 210 and 103 are quite weak for the samples crystallized below 110 °C. The zoomed-up profiles of the two strong reflections are depicted in Figure 4b. At $T_c < 120$ °C, an obvious change is found for the peak position of the 200/110 and 203 reflections. When 100 °C $< T_c < 120$ °C, the profiles of the 203 reflection can be resolved into two components originating from the α' and α phases, which suggests that the samples crystallized in this temperature range are the mixture of α' and α phases.

The half-width is also found to change depending on T_c . As a trial, the crystallite size is estimated on the basis of Scherrer's equation.²⁶ Figure 5a shows the T_c dependence of lattice spacing and crystallite size estimated for the 203 reflection. In the data analysis, the 203 reflection profile was separated into two components coming from the α' and α phases through the curve-fitting process. As the T_c is increased, the lattice spacing becomes smaller and therefore the chain packing becomes closer gradually. The half-width of the reflection becomes narrower, corresponding to the increase in the crystallite size (D_{203}). As already discussed in the previous paper,¹⁹ the α' form takes a disordered structure concerning the conformation and packing modes of the chains. The remarkable intensity increase and sharpening of many reflections during the crystallization even below 100 °C indicate a continuous and gradual enhancement of the structural regularity of the α' form, although the degree of ordering is far lower than that of the α form. As seen in Figure 5a, the size of α' crystallite increases with T_c below 100 °C. When the T_c is higher than 100 °C, the α crystallite starts to appear as already pointed out, but the domain size is small judged from the half-width of the α reflection. As the T_c is increased, the domain size of the α form is larger and the α' domain decreases instead, as illustrated in Figure 5b. Finally, the stable α form is formed at $T_c \geq 120$ °C, which is consistent with the previous DSC data. On the basis of the X-ray diffraction and DSC data, a kind of phase diagram concerning the α' and α forms has been constructed reasonably, as shown in Figure 3.

As shown in Figure 5, the lattice spacing of α' form decreases with increasing T_c at low temperature ($T_c < 100$ °C). It suggests that the α' form is a kind of metaphase rather than a stable

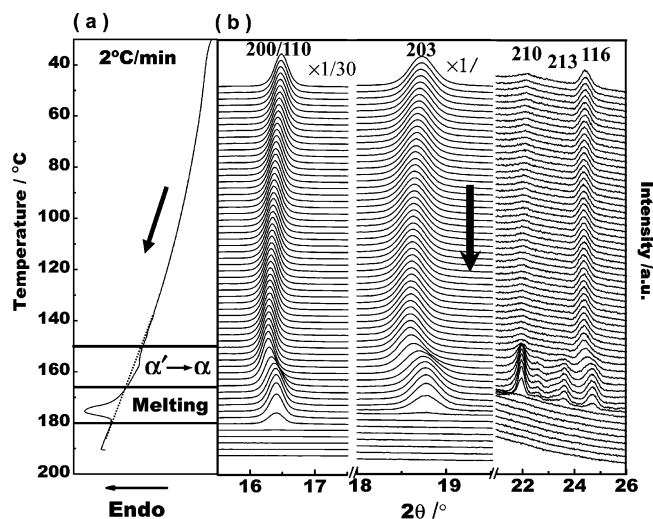


Figure 6. Simultaneous measurements of DSC (a) and WAXD (b) for the unoriented PLLA sample melt-crystallized at 90 °C (α' form). For clarification, different enlarge coefficients as indicated in the figure are used in different ranges of diffraction angles. Heating rate: 2 °C/min.

phase. Currently, it is not clear why the crystal structure of PLLA forms the disorder α (α') phase at low temperature ($T_c < 100$ °C). The morphology study by polarized optical micrographs (POM) shows that larger and more perfect spherulites and grainlike morphology appeared at high and low temperatures for the α' and α phases, respectively.¹⁶ By using TEM, the fibrillar crystallites with many sheaflike structure are observed clearly for α' form.⁸ In contrast, the stable α form demonstrates the lamellar morphology, and two chains are packed in the antiparallel mode in the unit cell.^{24,25} By considering that the very fast crystallization kinetics of PLLA caused by the higher nucleation rate at low temperature have been reported,^{10,11} we speculate that the disorder structure of α' form appears to rest on statistical upward-and-downward orientations of helical chains formed at low temperature with the distinct crystallization dynamics which are different from these of α form formed at high temperature. We need to investigate the crystallization mechanism of α' form in more concrete way, including molecular dynamics simulation, etc.

Simultaneous Measurement of WAXD and DSC. For disclosing the structural change in the small exothermic peak detected for the unoriented α' form, as shown in Figure 2, the simultaneous WAXD and DSC measurement was performed for the PLLA sample crystallized at 90 °C as an example. Figure 6 shows the result obtained at the heating rate 2 °C/min. With increasing temperature prior to the small exothermic peak, the peak position of the observed reflections shifts to lower angle side due to the thermal expansion of the lattice. In the temperature region of small exothermic peak, the 200/110 and 203 reflections shift remarkably toward the higher angle. Many sharp reflections start to appear, and the peaks of the α' phase disappear. As shown in Figure 7, the evolution of the overlapped WAXD profiles in the region of 18°–26° demonstrates such trend clearly. Of particular note, the apparent shifting of 203 and 116 reflections exhibits an isosbestic point, which is strong evidence that there is a first-order transition of the two phases (α' and α).

By the technique of curve fitting, the quantitative analysis of the intensity, half-width, and lattice spacing of the 203 diffraction of α' and α is made as shown in Figure 8 in comparison with the DSC data. Corresponding to the small exothermal peak, the intensity of α' phase decreases and that

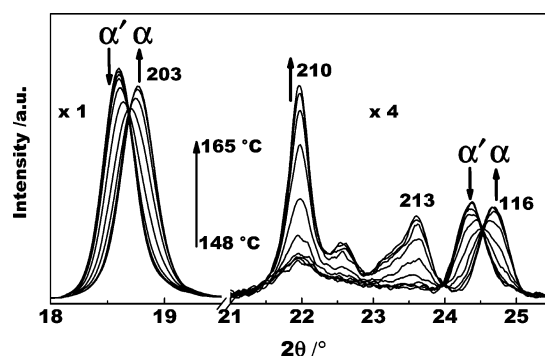


Figure 7. Overlapped WAXD profiles in the region of 18°–26° measured in the heating process from 148 to 165 °C (measured every ca. 2.4°), which is the temperature region of α' -to- α phase transition.

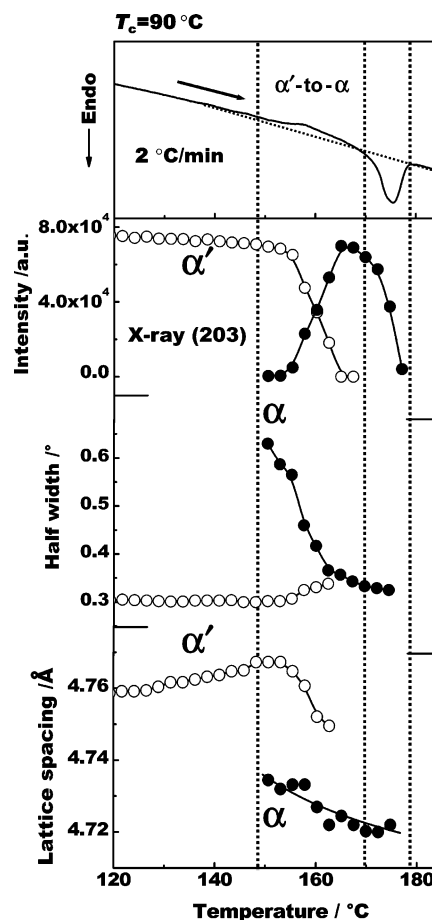


Figure 8. Temperature dependence of the intensity, half-width, and lattice spacing of the 203 diffraction of α' and α . For comparison, the corresponding DSC curve is displayed.

of α phase increases instead, which clearly suggests that the α' -to- α phase transition takes place. The inverse intensity change of 200/110 and 116 reflection (α' and α) and the appearance of the new reflection 210 (α) in this temperature region, as shown in Figure 9, also evidence this point. In the process of the α' to α phase transition, the half-width of α' phase increases gradually and that of α phase decreased remarkably. This change can be interpreted as discussed already in Figure 5b: the crystal domain of the α' phase decreases in number because of the generation of the α domain. At the beginning, the size of the newly born α domain is small. With the transition of α' to α , the α domain continues to grow and increases in size to give sharper X-ray reflection.

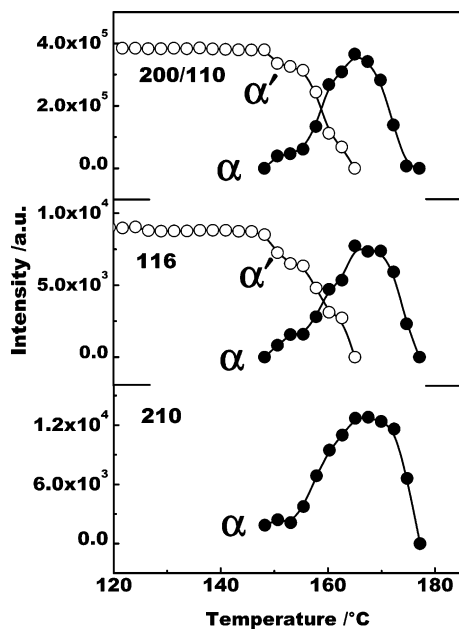


Figure 9. Temperature dependence of the intensity of the 200/110, 210, and 116 diffraction of α' and α .

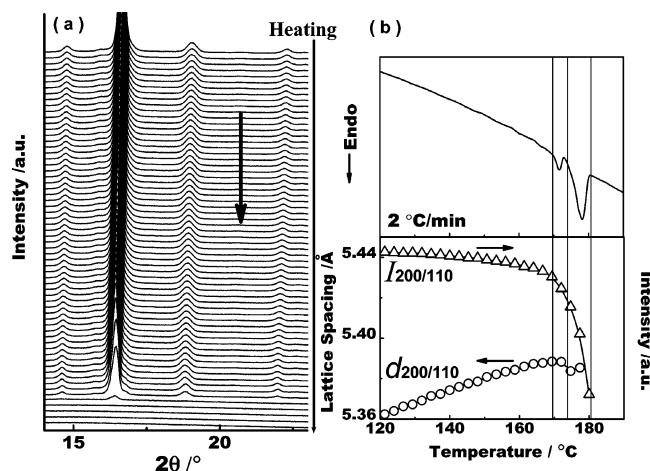


Figure 10. Simultaneous measurements of WAXD (a) and DSC (b) for the PLLA sample crystallized at 120 °C. For comparison, the plot of the diffraction angle and intensity of (200/100) as a function of the temperature is displayed in the bottom of (b).

In association with the α' -to- α phase transition, both of the lattice spacings of α' and α phases decrease slightly. It indicates that the chain packing of the remaining α' and newly generated α phase becomes more compacted. After completion of the α' -to- α phase transition, the α phase starts to melt with increasing temperature further, which corresponding to the melting peak well.

Simultaneous WAXD and DSC measurement was performed also for the sample crystallized at 120 °C, as shown in Figure 10a. This sample consists of the α phase and demonstrates the double melting behavior. A plot of the lattice spacing and the intensity of 200/110 reflection as a function of temperature is shown in Figure 10b. As pointed out already, this sample shows a subpeak (T_{m2}) below the main melting peak (T_{m1}) in the DSC thermogram. The relative crystallinity decreases obviously, and a very slight apparent lattice contraction appears corresponding to the temperature region of the subpeak. These changes are considered to reflect the characteristic melt-recrystallization behavior of α form itself.

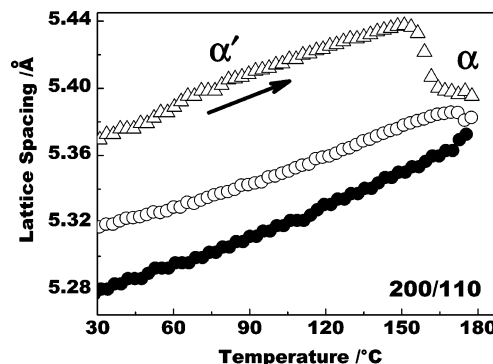


Figure 11. Lattice spacing changes of (200/100) diffraction of PLLA samples respectively crystallized at 90, 120, and 140 °C as a function of temperature.

Figure 11 compares the temperature dependence of the apparent lattice spacing ($d_{200/110}$) estimated for three kinds of samples crystallized at 90, 120, and 140 °C; the curve separation is not performed in this figure. The lattice spacing reaches essentially the same value at high temperature 170 °C, supporting the existence of two kinds of crystal modifications with different thermodynamic stability. The sample of $T_c = 90$ °C experiences the change from α' to α phase in the temperature region 150 °C, giving a remarkable change in $d_{200/110}$. The samples of $T_c = 120$ and 140 °C exhibit essentially the same behavior, although the lattice spacing becomes smaller for the sample crystallized at higher T_c . Anyway, it is important to notice that the lattice spacing reached at high temperature is essentially the same for these three samples.

Conclusion

In the present report, the thermal behavior of the various PLLA samples crystallized at the various T_c 's was investigated on the basis of WAXD and DSC measurements. It has been confirmed that the small exothermic peak in the DSC curve detected just prior to the melting peak is associated with the first-order-type disorder-to-order (α' -to- α) phase transition, as supported by the observations that the isosbestic points were found in the temperature-dependent WAXD profiles, and the observed reflections consist of two components of the α' and α phase as seen clearly for the higher 2θ reflections. As already reported, the X-ray fiber pattern keeps the high degree of chain orientation during the transition, indicating that the α' -to- α transition occurs in the solid state. The remarkable change in the half-width of the X-ray reflections corresponds to the change in the domain size between the α' and α phase regions, as illustrated in Figure 5b. These findings shed more light on the phase transition mechanism of the α' -to- α transition in a concrete way. The experimental confirmation of the existence of α' form is quite important in the interpretation of the various types of experimental data collected for the PLLA samples treated under the various thermal conditions.

Acknowledgment. This work was supported by MEXT "Collaboration with Local Communities" Project (2005–2009).

References and Notes

- (1) Dorgan, J. R. *Poly(lactic acid) Properties and Prospects of an Environmentally Benign Plastic*; American Chemical Society: Washington, DC, 1999; pp 145–149.
- (2) Ikada, Y.; Tsuji, H. *Macromol. Rapid Commun.* **2000**, *21*, 117–132.
- (3) De Santis, P.; Kovacs, J. *Biopolymers* **1968**, *6*, 299–306.
- (4) Hoogsteen, W.; Postema, A. R.; Pennings, A. J.; ten Brinke, G.; Zugenmaier, P. *Macromolecules* **1990**, *23*, 634–642.
- (5) Kalb, B.; Pennings, A. J. *Polymer* **1980**, *21*, 607–612.

- (6) Puiggali, J.; Ikada, Y.; Tsuji, H.; Cartier, L.; Okinara, T.; Lotz, B. *Polymer* **2000**, *41*, 8921–8930.
- (7) Cartier, L.; Okihara, T.; Ikada, Y.; Tsuji, H.; Puiggali, J.; Lotz, B. *Polymer* **2000**, *41*, 8909–8919.
- (8) Zhang, J. M.; Duan, Y. X.; Sato, H.; Tsuji, H.; Noda, I.; Yan, S.; Ozaki, Y. *Macromolecules* **2005**, *38*, 8012–8021.
- (9) Cho, T.-Y.; Strobl, G. *Polymer* **2006**, *47*, 1036–1043.
- (10) Di Lorenzo, M. L. *Eur. Polym. J.* **2005**, *41*, 569–575.
- (11) Di Lorenzo, M. L. *Polymer* **2001**, *42*, 9441–9446.
- (12) Abe, H.; Kikkawa, Y.; Inoue, Y.; Doi, Y. *Biomacromolecules* **2001**, *2*, 1007–1014.
- (13) Marega, C.; Marigo, A.; Di Noto, V.; Zannetti, R. *Makromol. Chem.* **1992**, *193*, 1599–1606.
- (14) Iannace, S.; Nicolais, L. *J. Appl. Polym. Sci.* **1997**, *64*, 911–919.
- (15) Myiata, T.; Masuko, T. *Polymer* **1998**, *39*, 5515–5521.
- (16) Mijović, J.; Sy, J. W. *Macromolecules* **2002**, *35*, 6370–6376.
- (17) Bras, A. R.; Viciosa, M. T.; Wang, Y. M.; Dionisio, M.; Mano, J. F. *Macromolecules* **2006**, *39*, 6513–6520.
- (18) Ohtani, Y.; Okumura, K.; Kawaguchi, A. *J. Macromol. Sci., Part B: Phys.* **2003**, *3–4*, 875–888.
- (19) Zhang, J. M.; Tashiro, K.; Domb, A. J.; Tsuji, H. *Macromol. Symp.* **2006**, *242*, 274–278.
- (20) Di Lorenzo, M. L. *J. Appl. Polym. Sci.* **2006**, *100*, 3145–3151.
- (21) Tsuji, H.; Ikada, Y. *Polymer* **1999**, *40*, 6699–6708.
- (22) Hoffman, J. D.; Weeks, J. J. *J. Res. Natl. Bur. Stand., Sect. A* **1962**, *66*, 13–34.
- (23) Brizzolara, D.; Cantow, H.-J.; Diederichs, K.; Keller, E.; Domb, A. J. *Macromolecules* **1996**, *29*, 191–197.
- (24) Aleman, C.; Lotz, B.; Puiggali, J. *Macromolecules* **2001**, *34*, 4795–4801.
- (25) Sasaki, S.; Asakura, T. *Macromolecules* **2003**, *36*, 8385–8390.
- (26) Guinier, A. *X-ray Diffraction*; W.H. Freeman: San Francisco, 1963; p 124.

MA0706071